

IAC-19-A6.6.4

REDSHIFT DISPOSAL MODULE FOR THE DESIGN OF END-OF-LIFE DISPOSAL TRAJECTORIES FOR LEO TO GEO MISSIONS

**Camilla Colombo¹, Gonzalo Vicario de Miguel², Despoina K. Skoulidou³,
Narcis Miguel Banos¹, Elisa Maria Alessi⁴, Ioannis Gkolias¹, Livio Carzana²
Federico Letterio², Giulia Schettino⁴, Kleomenis Tsiganis³, Alessandro Rossi⁴**

¹ Politecnico di Milano, Dep. of Aerospace Science and Technology, Milano, Italy; camilla.colombo@polimi.it

² Deimos Space SLU, Spain;

³ Aristotle University of Thessaloniki, Greece;

⁴ IFAC-CNR, Sesto Fiorentino, Italy.

Among its results, the ReDSHIFT project has developed a software tool for spacecraft operators, space agencies and research institutions to design the end-of-life of Earth-based missions and to study the interaction with the space debris environment. As part of this, the “Disposal Mapping” module, presented in this paper in its structure and algorithm, computes the end-of-life disposal strategy for missions whose operational orbit is in the orbital region from Low-Earth orbit to Geostationary Earth orbit. Given the initial orbit, the available Δv on board and the spacecraft characteristics in terms of cross area and mass, the options for end-of-life disposal are given and compared; namely, end-of-life disposal via one or a sequence of impulsive manoeuvres, end-of-life disposal through the use of a solar/drag sail or end-of-life through a hybrid sail plus an impulsive manoeuvre.

I. INTRODUCTION

Among its results, the ReDSHIFT (Revolutionary Design of Spacecraft through Holistic Integration of Future Technologies) project [1][2] has developed a software tool for spacecraft operators, space agencies and research institutions to design the End-Of-Life (EOL) of Earth-based missions and to study the interaction with the space debris environment [3]. As part of this, the “Disposal Mapping” module, presented in this paper in its structure and algorithm, computes the EOL disposal strategy for missions whose operational orbit is in the orbital region from Low-Earth Orbit (LEO) to Geostationary Earth Orbit (GEO). Given the initial orbit, the available Δv on board and the spacecraft characteristics in terms of cross area and mass, the options for end-of-life disposal are given and compared; namely, end-of-life disposal via one or a sequence of impulsive manoeuvres, end-of-life disposal through the use of a

solar/drag sail or end-of-life through a hybrid sail plus an impulsive manoeuvre.

This module is based on a study of the natural orbit evolution of many initial conditions in the low to medium and geostationary regions to identify long-term stable and unstable orbits to be used as graveyard or natural re-entry trajectories. The manoeuvre to reach such conditions from the operational orbit is calculated and compared with the available Δv on board the spacecraft at the EOL. Moreover, the re-entry can be enhanced through a sail. Different strategies for sail attitude control are compared and selected. The simpler solution is to deploy a passively stabilised sail or a balloon so that the attitude of the sail is always constant with respect to the Sun-Earth line. As a more advanced solution, in case control of the attitude of the sail can be ensured, a new modulating sail strategy is devised, that changes the attitude of the sail every six months, on average, to monotonically increase the orbit eccentricity and allow the use of solar sails also to higher altitude orbits in the Medium Earth Orbit (MEO) regime.

In the case a sail is used, the disposal mapping module also output the parameters for the technological design of the sail. Finally, a hybrid method is also proposed, where first a manoeuvre is given to move the spacecraft in a condition close to resonances, and then a sail is deployed. The disposal mapping module outputs all the available solutions given the operational constraints for the spacecraft to be then passed to the other modules of the software that assess the effect of this disposal on the space debris environment, and the demisability of the re-entry trajectory. The tool is integrated in the OpenSF simulation framework [4],[5]. All the results of the disposal mapping module have been validated with other available tools for orbit propagations and re-entry computation such as ESA DRAMA [6], OSCAR [7], DROMO [8] and STELA [9]. The paper is organised as follows: first the functional description of the module is given in Section II, then the module interfaces are described, focussing on the sub-modules and the connection with the other part of the software in Section III. This section provides a detailed description of the output files that will be generated by the disposal mapping module.

II. FUNCTIONAL MODULE DESCRIPTION

The “Disposal Mapping” module is aimed at providing the most convenient disposal strategy from different orbital regimes (LEO, MEO, GEO). To this aim, various end-of-life disposal strategies are computed and compared.

Based on the research in the ReDSHIFT project a number of maps of the orbit dynamics behaviour in the phase space have been computed indicating, for each orbital regime, the most convenient locations (in terms of the Keplerian orbital elements) where a spacecraft should be moved at the end-of-life, to minimise its residual orbital lifetime or, conversely, to maximise its stability in that

specific orbital altitude (e.g., in the case of the GEO graveyard orbits).

Namely, the disposal mapping module will perform the following tasks: (1) Provide the desirable manoeuvre to accelerate or improve the re-entry or graveyard injection; (2) Characterise the natural re-entry time or the stability of a graveyard orbit.

The module outputs the orbital parameters of the selected disposal orbits, along with the Δv of the manoeuvre required to reach the specific target orbit from the last operational orbit and the residual lifetime. The Δv computation can consider the possible use of area augmentation devices (when selected by the user), with a set area-to-mass ratio, namely, $A/m=1 \text{ m}^2/\text{kg}$. The optimal design of a deorbiting device (i.e. optimal choice of area-to-mass ratio and control strategy is instead performed by the sail sub-module)

Moreover, the module can output the ephemerides corresponding to all the selected disposal trajectories. The information on the final disposal trajectories is shared with the “Design for Demise Assessment” module, also part of the ReDSHIFT software to identify possible re-entry risks related to the selected trajectory and with the “Environmental Protection” module to compute the expected collisional flux on the disposed spacecraft along the selected disposal trajectory. The disposal mapping module calculations include:

- a database search algorithm to look through the space phase maps and to identify the proper disposal regions (given the selected inputs);
- a simple schematic orbital propagation algorithm to propagate the status of the spacecraft from the selected disposal status up to the desired residual lifetime.

The disposal mapping module first checks if the initial condition given by the user is reasonable, i.e. if the pericentre altitude is above the surface of the Earth, as

well as above the re-entry altitude (120 km). After this verification, it computes the Δv required to de-orbit directly to 120 km, i.e. the impulsive manoeuvre to lower the pericentre altitude to such value. If this cost is higher than the Δv on-board (according to the user input), then it starts the proper algorithm based on information that can

be obtained from the cartography of the circumterrestrial region [10],[12],[13],[14]. To this end, the module first discriminates the orbital regime of the input spacecraft orbit according to the criteria in Table 1. A dedicated algorithm computes the most convenient disposal strategies, as described in the following sections.

Table 1: Disposal mapping orbital regimes.

Regime	Semi-major Axis	Eccentricity	Inclination
GTO	21000 - 28000 km	0.5 - 0.8	3 - 8 deg, 26 - 31 deg, 43 - 49 deg, 61 - 66 deg
MEO	24500 - 30300 km	0.0 - 0.88	51 - 59 deg
GEO	41664 - 42665 km	0 - 0.3	0 - 90 deg
LEO	≤ 9378.137 km	10^{-4} - 0.28	≤ 120 deg

II.I. Low Earth orbit regime

The LEO disposal sub-module is based on the findings derived from the cartography described in [10], and aims, mainly, at defining the most convenient re-entry trajectory following such information [11]. The advantage of the strategy that will be explained in the following is that it is not dependent on the initial conditions grid set for the cartography.

The manoeuvre required to achieve a re-entry is computed based on the displacement in semi-major axis a , eccentricity e and inclination i which ensures an atmospheric re-entry. These target conditions are derived from the cartography. The equations needed to move to the desired orbit are the inverse of the following Gauss' planetary equations:

$$\begin{aligned}\Delta a &= 2 \frac{e \sin(\nu)}{n \sqrt{1-e^2}} \Delta v_r + 2 \frac{1 + e \cos(\nu)}{n \sqrt{1-e^2}} \Delta v_t \\ \Delta e &= \frac{\sqrt{1-e^2} \sin(\nu)}{na} \Delta v_r \\ &\quad + \sqrt{1-e^2} \frac{\cos(\nu) + \cos(E)}{na} \Delta v_t \\ \Delta i &= \frac{r}{h} \cos(u) \Delta v_h\end{aligned}$$

where the target displacements are $(\Delta a, \Delta e, \Delta i)$, the radial, transversal, out-of-plane components of the manoeuvre are $\Delta v = (\Delta v_r, \Delta v_t, \Delta v_h)$, ν is the true anomaly, E the eccentric anomaly, u the argument of latitude, r the radius, h the angular momentum, n the mean motion.

The algorithm implemented looks for two kinds of re-entry solutions, namely,

- the so-called *non-resonant solutions*: the re-entry is driven by the effect of the atmospheric drag, and thus, the target conditions are only semi-major axis and eccentricity (i.e. $\Delta v_h=0$ km/s);
- the so-called *resonant solutions*: the re-entry can occur because of the combined effect of atmospheric drag and a different orbital perturbation. In this case, the target conditions include also the inclination value.

For both types of solution, the algorithm provides the user with the minimum-cost one and compares it with the available Δv on-board. In both cases, if the Δv computed is lower than the one available, then the algorithm computes the displacement in Ω , ω due to the same manoeuvre, using the following equations:

$$\Delta \Omega = \frac{r \sin(u)}{h \sin(i)} \Delta v_h$$

$$\Delta\omega = -\frac{\sqrt{1-e^2}}{aen}\cos(v)\Delta v_r + \frac{2\sqrt{1-e^2}}{aen(1+ecos(v))}\sin(v)\Delta v_t - \frac{rsin(u)}{hsin(i)}\cos(i)\Delta v_h$$

Such a refined target condition is propagated to verify that the re-entry time is lower than the requested value (10 or 25 years depending on the input and on the type of solution), and to compute the ephemerides and final conditions at re-entry needed by the environmental protection and design for demise assessment modules. If the Δv computed is higher than the one available on-board, in the case of non-resonant solutions or resonant solutions with $A/m=1 \text{ m}^2/\text{kg}$, the algorithm provides the information on the minimum Δv required to achieve a re-entry.

In any case, the algorithm also computes the cost to move to a graveyard orbit beyond 2000 km of altitude.

For the non-resonant case, the target conditions in semi-major axis and eccentricity to have a re-entry have been derived from numerical simulations considering the effects of orbit zonal harmonics, atmospheric drag, solar radiation pressure, lunisolar gravitational perturbations.

Two possible values of the residual lifetime were defined, 25 years and 10 years, respectively. The results for both area-to-mass ratios selected are shown in Fig. 1, on the left, the required eccentricity as a function of the semi-major axis and, on the right, the pericentre altitude h_p as a function of the semi-major axis are depicted. The (a, e) configurations are the target conditions for the non-resonant re-entry disposal strategy.

In the resonant case, a difference is made between the low and the high area-to-mass ratio cases to identify the

re-entry target conditions. In both cases, the target conditions are (a, e, i) configurations associated with a re-entry in less than 25 years.

Without an area-augmentation device, the re-entry is achieved by means of the combined effect of the atmospheric drag and a different perturbation, which can be of various nature. The target conditions have been obtained experimentally by analysing the re-entry time associated with all the initial conditions. The cases complying with a 25-year re-entry have been selected and listed in a single file. With a sail, instead, the dominant resonant corridors are associated only with the solar radiation pressure and their location can be found semi-analytically [15]. In particular, the target conditions are associated with the following condition:

$$\dot{\psi} = n_1\dot{\Omega} \pm \dot{\omega} \pm n_S \cong 0$$

where the rate of precession of the longitude of the ascending node and the argument of pericentre are assumed to be due only to the oblateness of the Earth and to be function of (a, e, i) , n_S (i.e. the mean motion of the Sun), and n_1 (always equal to 0 or 1). The resonant values of inclination and semi-major axis are tabulated for values of eccentricities in the LEO region and used as database for the software. Moreover, to ensure that these configurations are associated with a variation in eccentricity high enough to achieve a re-entry, a simplified analytical theory is applied to estimate the maximum eccentricity variation Δe_{SRP} that can be obtained [15].

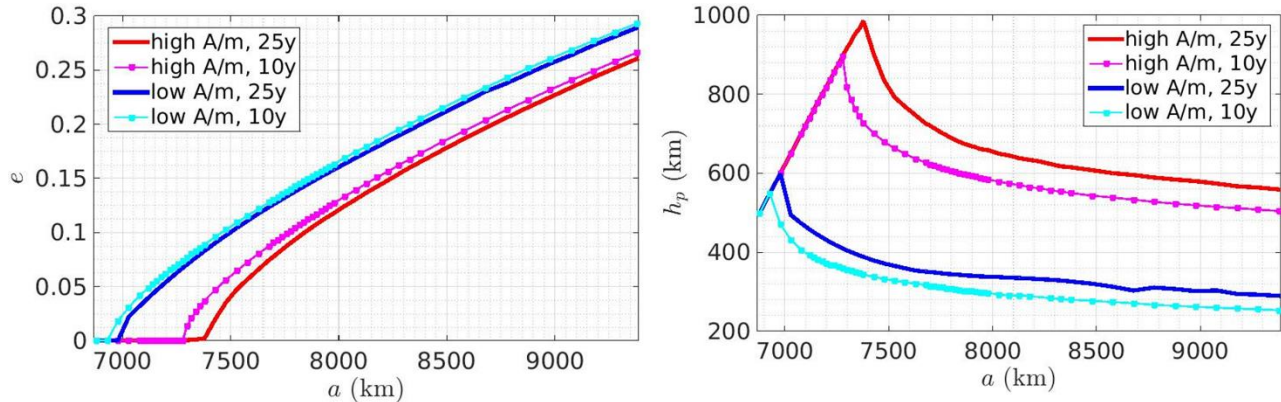


Fig. 1. Target conditions for non-resonant re-entry for the LEO regime.

II.II. Medium Earth orbit and geostationary transfer orbit regime

A focus in the medium Earth orbit regime is given to the Global Navigation Satellite System (GNSS) region and Geostationary Transfer Orbits (GTOs). For GNSS orbits, two possibilities for post-mission disposal are considered:

- Transfer to a neighbour orbit that eventually results in re-entry via eccentricity growth (i.e., re-entry solutions)
- Transfer to a neighbour orbit that is long-term stable and has no interference with operational orbits (i.e., graveyard solutions)

For the highly eccentric MEO orbits, i.e. GTOs, and Highly Elliptical Orbits (HEOs) only re-entry solutions are considered, as they are abundant in the region and easily accessible (i.e. with a low Δv) by a simple manoeuvre.

For any given initial orbit, O1 (i.e. the satellite's orbit at the end of its operational period), a search for conditionally-optimal disposal solutions is performed in a

data-base, which contains a large set of pre-computed possible solutions, using the strategy discussed in [12],[16]. Similarly with what is done for the GEO region, Gauss's planetary equations are used to define reachability domains, for a representative sample of "O1" orbits in the entire MEO region, and for a given maximum, on-board Δv . A Δv up to 1 km/s was considered, although a cost of $\Delta v \sim 100$ m/s is closer to being acceptable for re-entry solutions, while a typical graveyard solution requires much less than that.

As shown in Fig. 2, a change in inclination of order 1 degree requires a Δv of around 100 m/s. Therefore, in order to maximise reachability in (a, e) and increase the number of possible re-entry solutions around O1, we restricted ourselves to co-planar transfers as a first approximation. For sake of simplicity, we considered two possible types of manoeuvres that the satellite can execute: (i) single-burn manoeuvres and (ii) two-burn, bi-elliptic manoeuvres, between co-axial ellipses (i.e. for the same value of ω , or for $\omega' = \omega + \pi$); two-burn transfers turned out to be less expensive in Δv [16].

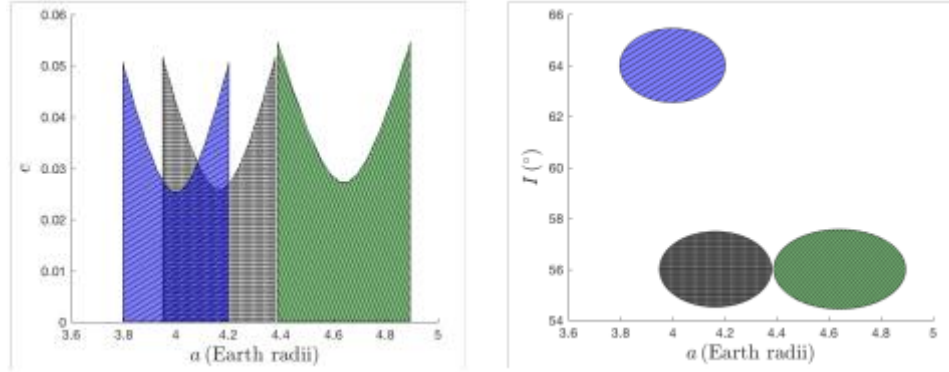


Fig. 2. Reachability zones for GNSS orbits (left) in (a, e) and (right) in (a, i) .

All possible re-entry solutions found in the dynamical study in [16] have been stored in a data-base and hence can be retrieved from the MEO software sub-module, when applicable. The same holds true for all graveyard solutions found, defined in [16] as orbits lying within 500 km from each GNSS constellation's nominal location that: (i) are stable for 200 years, and (ii) keep their eccentricity so small that no crossing occurs within a 50 km tolerance region around any of the GNSS locations within 200 years (i.e. no interference) as shown in Fig. 3. The possible re-entry/graveyard orbits that respect the rules set herewith, are what we define as conditionally optimal solutions.

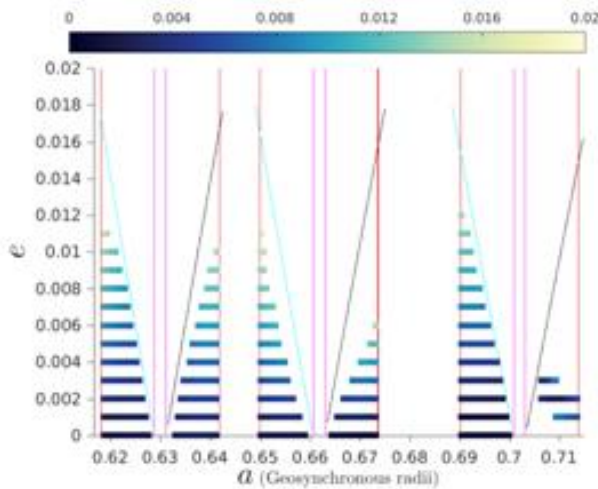


Fig. 3. Definition of graveyard zones around the Global Positioning System, Beidou and Galileo constellations and distribution of stable graveyard orbits found in (a, e) for $i=56$ deg.

The MEO disposal software sub-module works as follows: for each 'O1' orbit that the user defines (within the specified orbital elements regions), the software selects its 'nearest neighbour' from our grid, on the corresponding dynamical 'map'. Then, given the maximum Δv input by the user, the algorithm:

- Searches the database for all possible EOL solutions, according to the rules set above.
- Outputs the corresponding dynamical lifetime map from the database: this map shows the time needed for all possible re-entry solutions to re-enter.
- Computes the map of re-entry time, t , versus Δv and the corresponding Pareto Fronts for single- and two-burn manoeuvres, starting from O1.
- For re-entry solutions derives the 'optimal' solutions in terms of 'dwell time' (t) and 'cost' (Δv) and displays all relevant info (elements, Δv , t) to the user.
- Generates scripts, for plotting the ephemeris of the optimal solutions.
- Repeats steps b – e for graveyard orbits, if O1 is in the GNSS region, outputs the corresponding maximum eccentricity map from the database, computes the map of maximum eccentricity, e_{\max} , versus Δv and the corresponding Pareto Fronts for two-burn manoeuvres, starting from O1, and derives

the ‘optimal’ solutions in terms of ‘cost’ (Δv) and displays all relevant info (elements, Δv , t) to the user.

- g. For re-entry solutions, retrieves re-entry conditions at 120 km from Earth’s surface, to be passed to the Design for Demise routine.

II.III. Geostationary orbit regime

In the GEO region, for a given post-mission orbit there exist three options:

1. to transfer to a neighbourhood orbit which over the long term will result in a re-entry via eccentricity growth,
2. to transfer to a neighbourhood orbit which will be stable over the long term,
3. do not to perform any transfer and let the spacecraft orbit naturally evolve towards re-entry or towards a stable graveyard orbit.

The third option is usually not a viable solution for geosynchronous satellites, mainly due to the geosynchronous protected region. Therefore, we will concentrate in the other two options, namely the graveyard and re-entry design.

The method used for calculating the optimal disposal orbit for a given initial post-mission condition consists of three main steps and a schematic representation of the work-flow is given in Fig. 4. In the following we describe in detail each step of the disposal design process [17],[18],[19].

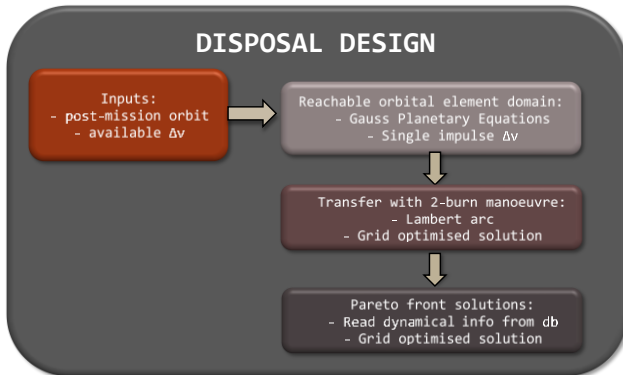


Fig. 4. Flowchart of the disposal design process.

Step 1: Reachable orbital element domain

Given a maximum available Δv_{max} the reachable space in orbital elements $\Delta \alpha$ is calculated, where $\alpha = [a, e, i, \Omega, \omega]$. This is done via an instantaneous impulsive manoeuvre by means of Gauss’s equations written in finite differences form,

$$\begin{aligned}\Delta a &= \frac{2a^2 v}{\mu_E} \Delta v_t \\ \Delta e &= \frac{1}{v} \left(2(e + \cos v) \Delta v_t - \frac{r}{a} \sin v \Delta v_n \right) \\ \Delta i &= \frac{r}{h} \cos(v + \omega) \Delta v_h \\ \Delta \Omega &= \frac{r \sin(v + \omega)}{h \sin i} \Delta v_h \\ \Delta \omega &= \frac{1}{ev} \left(2 \sin v \Delta v_t + \left(2e + \frac{r}{a} \cos v \right) \Delta v_n \right. \\ &\quad \left. - \frac{r \sin(v + \omega) \cos i}{h \sin i} \Delta v_h \right)\end{aligned}$$

where $\Delta v_t, \Delta v_n, \Delta v_h$ is the finite change in velocity in the tangential, normal and out-of-plane direction, so that

$$\begin{aligned}\Delta v_t &= \Delta v \cos \alpha \cos \delta_{max} \\ \Delta v_n &= \Delta v \cos \alpha \sin \delta_{max} \\ \Delta v_h &= \Delta v \sin \alpha_{max}\end{aligned}$$

where $0 \leq \alpha < 360^\circ$ and $-90^\circ \leq \delta \leq 90^\circ$ are the right ascension and co-declination that describe the orientation of the Δv manoeuvre with respect to the t-n-h frame. The reachable domain is then defined as:

$$\begin{aligned}\alpha_{0min} &= \alpha_0 - \Delta \alpha \\ \alpha_{0max} &= \alpha_0 + \Delta \alpha\end{aligned}$$

removing the values which are not physically possible (e.g. $e < 0$). As an example, Fig. 5 shows the shape of the reachable element domain for a circular orbit in the GEO region.

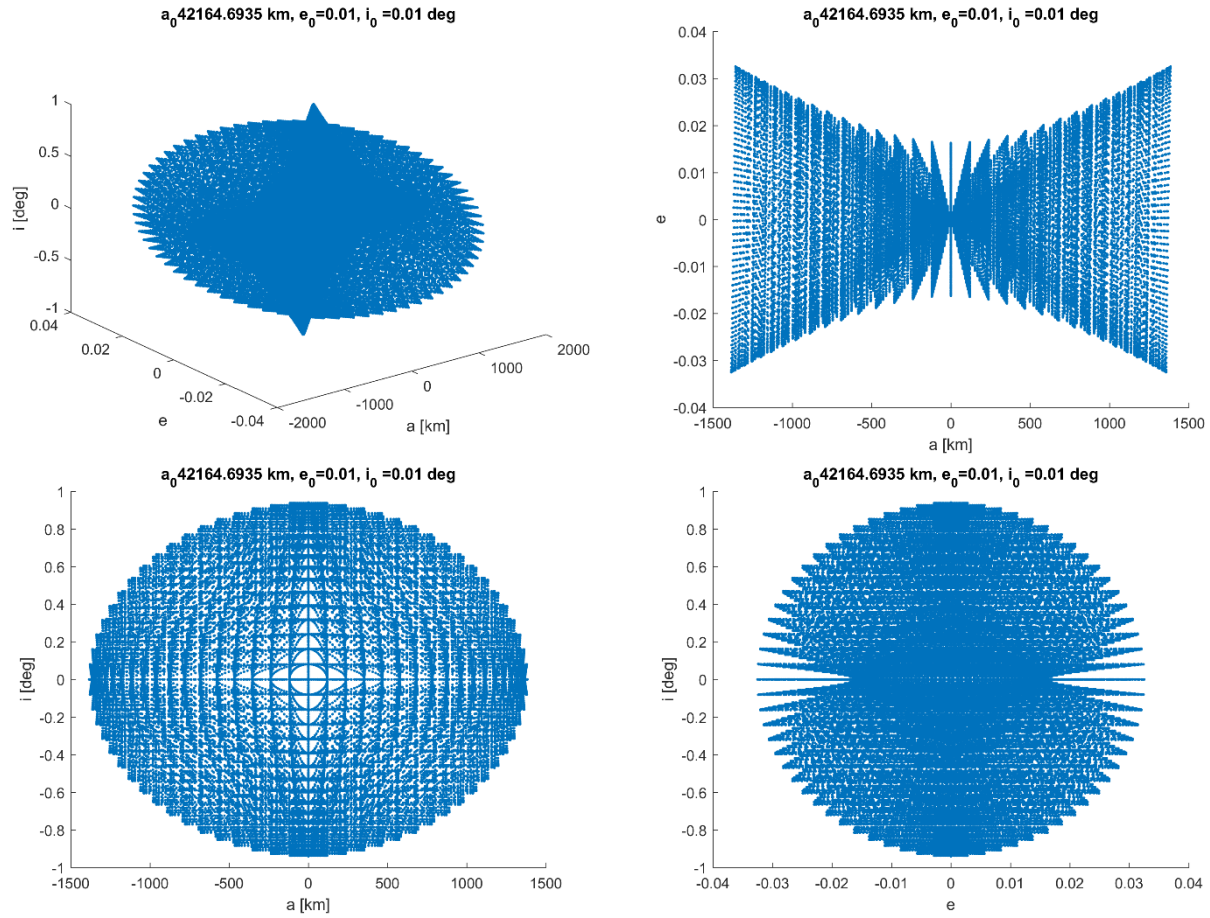


Fig. 5. Reachable orbital element domain starting from a post-mission initial orbit with $a = 42165$ km, $e = 0.01$, $i = 0.01$ deg, $\Omega = 0$ deg and $\omega = 0$ deg.

Step 2: Optimal two impulse transfer

The second step consists of calculating the required Δv to reach any orbit belonging to the reachable domain. To this aim, the Lambert algorithm is used. A grid in time of flight for the Lambert algorithm is defined with a step of ΔToF in the domain $[0, \text{ToF}_{\max}]$; given the five orbital elements on the initial orbit and the target orbit, the true anomaly on the two orbits are also determined via a grid search with a step of Δf , where f is the true anomaly. For each point in this three-dimensional grid a Lambert arc is

calculated from the initial to the target orbit and the total Δv is calculated as

$$\Delta v = \|\mathbf{v}_{\text{transfer}_0}(f) - \mathbf{v}_0(f)\| + \|\mathbf{v}_{\text{target}}(f) - \mathbf{v}_{\text{transfer}_0}(f)\|$$

where the dependence on the true anomaly f is shown. The minimum Δv to reach each of the reachable target orbits is stored.

Step 3: Pareto front

At this point the next step is to select among them the best disposal strategy through re-entry or graveyard. Each target orbit corresponds to a different long-term evolution, which in some cases may lead to re-entry within the 120-year. To quickly characterise the long-term evolution of

each target orbit two parameters are recovered from the dynamical maps database

- the maximum variation of eccentricity over the 120-year period

$$\Delta e = e_{max}(t) - e_{min}(t) \quad t \in t_0 + [0, 120 \text{ year}]$$

- the total time Δt of the long-term evolution which is equal to 120 years if the orbit does not decay but is lower in case the orbit re-enters via eccentricity growth.

These two parameters are used to filter and sort the best disposal. In order to identify the relevant solutions, the Pareto Front of the solutions $\Delta v - \Delta e$ is calculated for the graveyard disposal, while the Pareto Front of the solutions $\Delta v - \Delta t$ is calculated for the re-entry disposal.

As an example, Fig. 6 from [18] shows an example of the solution found for a graveyard disposal starting from α_0 and a re-entry disposal starting from α_0 . The grey points are all the solution found, the red points are the solutions belonging to the Pareto Front. The red solutions represent the front of the solutions that minimises the required Δv and the corresponding variation of eccentricity Δe for graveyard orbits or the corresponding Δt , i.e. time for re-entry for re-entry orbits.

For each of the solutions belonging to the graveyard or the re-entry Pareto front the transfer characteristic are stored, i.e. Δv magnitude and direction for the Lambert arc and position on the initial and target orbit where the two impulsive Δv should be given.

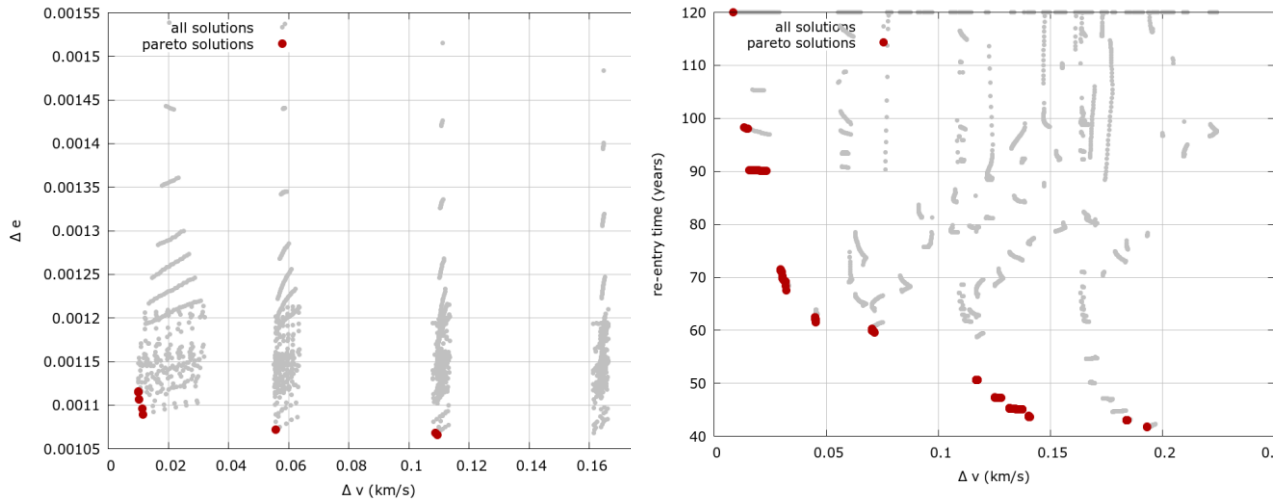


Fig. 6. Reachable orbital element domain starting from a post-mission initial orbit with $a = 42165$ km, $e = 0.01$, $i = 0.01$ deg, $\Omega = 0$ deg and $\omega = 0$ deg.

II.IV. Sail sub-module

The aim of this sub-module is twofold: provided some operational orbit data, spacecraft mass and cross area, and maximal time to deorbit; first, to assess the feasibility of the passive or modulating strategies for deorbiting a spacecraft for the input data, and second, to assess the feasibility of the construction of such a spacecraft structure with the current technological constraints. Here both deorbiting strategies are described, after that a description

of how the sail sub-module operates to choose between them two is provided, and this section finishes with the explanation of the feasibility test for the input sail data.

Passive deorbiting

The so-called passive deorbiting strategy was introduced in [20] consists of exploiting the counter-intuitive idea of ‘spiralling outwards’ by increasing the orbit eccentricity. Note that since the perigee radius is related with the eccentricity and semimajor axis by $r_p =$

$a(1 - e)$, for fixed a (that is a feature of adequately averaged equations of Earth satellite motion) an increase of e produces a decrease of r_p . In [20], the J_2 problem perturbed by solar radiation pressure SRP is considered. The applicability of this method further requires an attitude assumption: the sail has to be a reflective flat plate whose normal is parallel and in the same sense as the Earth-Sun vector. In that case, each value of the semi-major axis gives rise to a distinct evolution of the eccentricity along the orbits, and in some cases the perigee radius of spacecraft initially in circular orbit can deorbit in a prescribed amount of time by just deploying a sail as described facing the sunlight during all its orbit. But it can happen that for some values of a , on the one hand, the increase in eccentricity may not be enough to deorbit, or even if it is theoretically feasible the required deorbit time exceeds the established time limits.

Modulating deorbiting

A related deorbit strategy that involves minimal attitude control is the so-called active strategy, that was introduced in [21]. This strategy consists of ‘spiralling inwards’ towards the Earth by producing a decrease in the semi-major axis of the orbit. For a setting as before, the authors of the cited article suggest maximising the SRP acceleration when travelling towards the Sun and minimizing it when travelling away from it. In [14] this strategy was compared to the passive one explained in the previous subsection concluding that the passive was superior in performance. Based on these findings, a new sail control strategy was proposed, named modulating control strategy, that changes the attitude of the sail, making it perpendicular or at feather to the Sun direction every six months, to keep increasing the orbit eccentricity. As an example Fig. 7 shows the requirements in terms of effective area-to-mass ($c_R A/m$) for a 25-year deorbiting

time with modulating solar radiation pressure strategy. The colour bar represents the required effective area-to-mass.

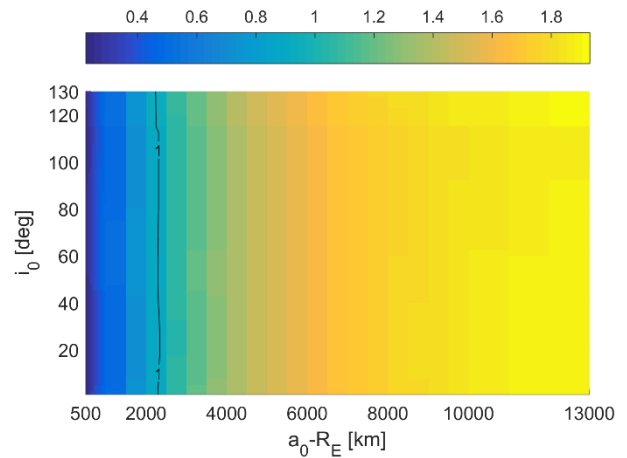


Fig. 7. Requirements in terms of effective area-to-mass ($c_R A/m$) for a 25-year deorbiting time with modulating solar radiation pressure strategy. The colour bar represents the required effective area-to-mass.

Deorbiting strategy selection

The selection of deorbiting strategy consists of first testing whether the passive deorbiting approach is feasible in the prescribed time if we start in the provided operational data. In case it is feasible, the sub-module tests whether a sail with the input area and spacecraft mass specifications is constructible with the current technological boundaries and outputs the results. The constructability assessment is addressed in the next subsection. In case the passive approach is not enough, the same deorbiting problem is studied using the modulating control strategy, and in case that deorbiting is feasible the sub-module tests the constructability outputs the results.

The output, in case any of the two strategies is enough to deorbit the spacecraft under consideration, consists of maps that aim to characterise the sail requirements provided the given operational orbit, and some data, that include the constructability requirements, conditions at 120 km and which control strategy was used to obtain successful results. If the disposal is feasible but the sail is not constructible, the sub-module provides the maximum

possible specifications considering the available technology and the corresponding map where to locate that result. Fig. 8 shows the flowchart of the sail dynamics module.

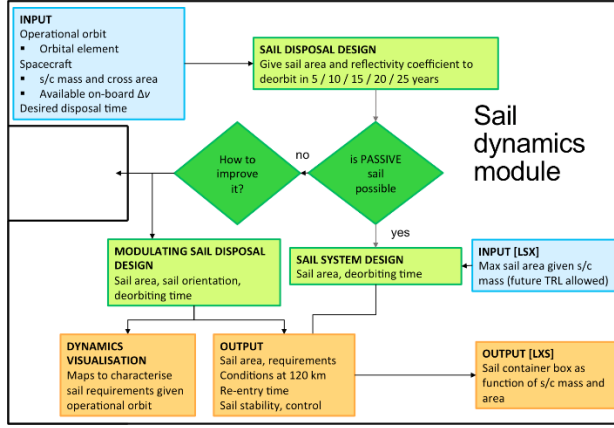


Fig. 8. Flowchart of the sail disposal module.

Sail technology feasibility

The constructability of the input sail data is assessed as suggested in [22]. To do so, one considers a squared drag sail with side length L . The ideal sail mass m_{DRS} , according to the cited contribution depends on L in a linear way, and on the chosen boom technology. There are two options, for different mass range of the spacecraft:

1. T_1 : Small, Light, that applies for spacecrafts of at Most $m_{sc} \leq 100$. The maximal achievable area in this technology is that of Neoscout mission, 86 m^2 . In this case

$$m_{DRS}(L) = aL + b, \quad a = 0.35, b = 0.39.$$

2. T_2 : Large, Heavy, that applies for spacecraft of mass bounded by $100 \leq m_{sc} \leq 1000$. The maximal achievable area in this technology is that of Drag sail GNC - LuxSpace project, of 450 m^2 . In this case,

$$m_{DRS}(L) = aL + b, \quad a = 1.42, b = 3.79.$$

Given a mass of the spacecraft m_{sc} the sub-module provides the required area-to mass ratio σ to deorbit the

spacecraft in less than a prescribed time also provided by the user. This ratio σ decomposed as

$$\sigma = \frac{A}{m_{sc}} = \frac{\eta L^2}{m_{sc} + m_{DRS}(L)}$$

where we denoted $A = \eta L^2$, the effective area of the sail sub-module, being $\eta = 0.92$, the percentage (technological) of the total area which is not empty space. Note this last equation is a quadratic equation that can be solved explicitly, and the solution we are interested in reads

$$L = \frac{a\sigma + \sqrt{\sigma(a^2\sigma + 4\eta(b + m_{sc}))}}{2\eta}$$

This reasoning is applied to decide whether the input spacecraft mass and area are feasible according the current technological constraints. When the sub-module assesses this part, it returns the product of the reflectivity coefficient c_R times area-to-mass ratio in the ideal case (using that previously provided by the sub-module) and considering the technological constraints.

III. MODULE INTERFACES

The organisation of the sub-modules of the disposal mapping module is shown in the schema in Fig. 9. For a given set of input both the computation of the sequence of Δv manoeuvres and the design of the sail for disposal are performed.

Firstly, the properties of the sail are computed via the sail technology sub-module, which are later used by the other sub-modules. After that, in parallel, the sail disposal and the manoeuvre disposal options are computed to be compared. The sail disposal sub-module computes the disposal solutions considering the deorbiting time requested by the user and compare the sail requirements to the one achievable by the current technology through the sail technology sub-module. Parallely, the sub-module corresponding to the orbital regime given as input (LEO, GEO or MEO) computes the disposal orbits considering two fixed values of area to mass ratio (a lower value of

0.012 m²/kg and a higher value of 1.0 m²/kg). All five disposal sub-modules generate ephemeris re-entry interface point files that are the inputs of the “Flux and Collision Probability” module and design for demise assessment module, respectively.

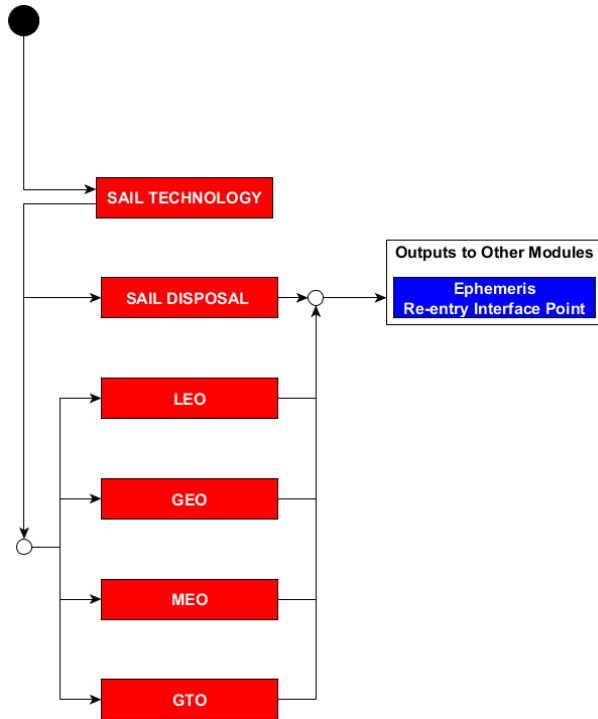


Fig. 9. Interaction between disposal mapping sub-modules.

III.I. Input

A configuration file of the disposal mapping module defines the characteristics of the spacecraft to be analysed in terms of orbit definition, total Δv available on-board, mass and disposal options. Table 2 provides a full description of all the parameters contained in the configuration file. The orbital elements are referred to the Earth equatorial plane.

III.II. Output

The disposal mapping module can generate different set of outputs given different input conditions and different disposal strategies.

Re-entry iinterface conditions

The disposal sub-modules (i.e. sail disposal, LEO, MEO and GEO) generate a file called that contains the orbit condition at 120 km when a re-entry solution is reached. This output is used as input for the design for demise assessment module. The conditions are given as: label identifying the scenario, mass (kg) and area of the spacecraft (m²), a (km), e , i (deg) computed at 120 km.

Table 2. Disposal mapping configuration file parameters.

Parameter	Description	Type	Units	Valid Range
sma	Semi-major axis	Float	km	0 – 42665
ec	Eccentricity	Float	N/A	0 – 1
inc	Inclination	Float	degrees	0 – 120
RAAN	Right Ascension of the Ascending Node	Float	degrees	0 – 360
w	Argument of Pericentre	Float	degrees	0 – 360
dv	Maximum Δv on board	Float	m/s	≥ 0
SAIL	Solar sail presence	Boolean	N/A	TRUE or FALSE
tor ¹	Re-entry time: 10 or 25 years	Integer	years	10 or 25
epoch	Epoch: 1 \rightarrow 22.74/12/2018, 2 \rightarrow 21.28/06/2020	Integer	N/A	1 – 2
mass	Satellite mass	Float	kg	0 – 1000

¹ The re-entry time can assume either the value 10 or 25 years, this input is used only for the LEO and the sail design sub-module not for the MEO and GEO sub-modules which can use any value of the deorbiting time.

Ephemeris files

The disposal sub-modules (i.e. sail disposal, LEO, MEO and GEO) generate the trajectory ephemerides for each feasible disposal solution (i.e., resonant orbits, direct re-entry orbits, graveyard orbits, etc.). The corresponding ephemerides down to 120 km of altitude at a time step of 10 days are computed. The ephemerides file contains the time in MJD, the five slow-moving orbital elements (a , e , i , Ω , ω), the area-to-mass A/m , the spacecraft cross-area and mass. The units are km, deg, m², kg. These files are used as input by the flux and collision probability module.

ASCII output files

The LEO sub-module can provide the following output files:

- The list of feasible re-entry solutions, according to the user initial choice. The feasible solutions are given in terms of initial epoch, Δv required, target initial conditions, usage of the sail.
- ephemerides files containing time and orbital element evolution (a , e , i , Ω , ω , M), A/m , area, mass. For each feasible re-entry solution, the corresponding ephemerides are provided up to 120 km of altitude.
- For the non-resonant solutions, the change in (a , e) due to a given Δv , applied at a given value of true anomaly ν . This manoeuvre is the one needed to exploit the effect of the atmospheric drag to achieve a re-entry.
- For the resonant solutions, only in the case of $A/m=1$ m²/kg, it is provided the change in (a , e , i) due to a given Δv applied at a given value of ν . In this case, the manoeuvre is aimed at exploiting the effect of the solar radiation pressure and Δe_{SRP} is a first estimate of the variation in eccentricity caused by the perturbation.
- The minimum value of Δv (m/s) for re-entry for each resonance.

The MEO sub-module can provide the following output files:

- Files including all information needed to generate the dynamical lifetime (t) versus Δv diagrams for the re-entry solutions. The first files correspond to single-burn transfers, whereas the second ones correspond to two-burn (Hohmann-like) transfers.
- Data files contain all information needed to generate the Pareto fronts, for the single- and two-burn transfers, respectively (re-entry solutions).
- Data files include all information needed to generate the maximum eccentricity (e_{max}) versus Δv diagrams for the graveyards, corresponding to two-burn transfers.
- Data files include all information needed to generate the pareto front for the graveyard solutions.

The GEO sub-module provides the following outputs (for more information on the output see also [13][17][18][19]:

- A file containing all the possible manoeuvres computed during the execution of the disposal module. The information contained is: target orbit ID in the database, Δv to reach the target orbit in km/s, eccentricity variation of the target orbit, lifetime of the target orbit in years.
- A file containing the Pareto front solutions for the case of the graveyard disposal design. The information contained is: target orbit ID in the database, Δv to reach the target orbit in km/s, eccentricity variation of the target orbit, lifetime of the target orbit in years.
- A file containing the target orbital elements for the pareto front solutions for the case of graveyard disposal design. The information contained is: semi-major axis of the target orbit in km, eccentricity, inclination in degrees, RAAN in degrees, perigee in degrees, Δa variation of the semi-major axis in km, Δe variation of the eccentricity and lifetime in years.

- A file containing the Pareto front solutions for the case of the re-entry disposal design. The information contained is: target orbit ID in the database, Δv to reach the target orbit in km/s, eccentricity variation of the target orbit, lifetime of the target orbit in years.
- A file containing the target orbital elements for the pareto front solutions for the case of graveyard disposal design. The information contained is the semi-major axis of the target orbit in km, the eccentricity, the inclination in degrees, the RAAN in degrees, perigee in degrees, the Δa variation of the semi-major axis in km, the Δe variation of the eccentricity and lifetime in years.

The sail disposal sub-module provides an output file with the following information:

- Scenario
- Sail area [m²]
- Sail mass [kg]
- Area-to-mass ratio [m²/kg]
- Technological limiting sail area [m²]
- Technological limiting sail mass [kg]
- Technological limiting area-to-mass ratio [m²/kg]
- Membrane percentage [%]
- Boom percentage [%]
- Empty percentage [%]

Gnuplot driver files

For LEO, the gnuplot scripts are conceived to generate figures to show, in case of re-entry solutions:

- The evolution in time of a , e , i ;
- The Δv cost to target a given (a, e) or (i, a) condition. The latter case is considered only in the case of $A/m=1$ m²/kg, when it is also possible to depict the estimated variation in eccentricity due to the perturbation.

For the MEO regime, the generated gnuplot scripts allow to generate figures, showing:

- The lifetime- Δv diagram and the Pareto fronts for the re-entry solutions

- The e_{\max} - Δv diagram and the Pareto front for the graveyards
- The time evolution of the orbital elements $(a, e, i, \Omega, \omega)$ of the conditionally-optimal disposal orbits found (of each type).

For the GEO region, the generated gnuplot scripts allow to generate figures to plot:

- The Pareto front for the graveyard design case.
- The Pareto front for the re-entry design case.
- The orbital evolution of the selected disposal orbits.

The module also provides a gnuplot script to plot the evolution of the Keplerian elements $(a, e, i, \Omega, \omega)$ as a function of time. This allows on-line visualisation and output of the generated plots in png format.

IV. WEBTOOL INTERFACE

As the whole ReDSHIFT tool, the disposal mapping has also a web interface available at <http://redshift-h2020.eu/>. The disposal mapping web interface contains two tabs, the “Orbit” and “Disposal” ones, which open two pop-up windows. In the orbit configuration window one can select the orbital regime available options (GTO, GNSS, GEO, LEO). Concerning the other parameters, these can be directly written in the corresponding boxes through the keyboard. As for the disposal configuration window, the only values the user can directly input through keyboard are the maximum Δv on board and mass parameters. Apart from these, it is possible to choose whether a sail is present or not on-board the spacecraft. Eventually, it is possible to navigate through the available options of the re-entry time

V. CONCLUSION

This paper described the functionalities and interfaces of the disposal mapping module of the ReDSHIFT tool. This module can be freely used in its online version to compute the disposal strategy for spacecraft in LEO, MEO

or GEO orbit via impulsive manoeuvres or though the deployment of solar sails.

ACKNOWLEDGMENTS

The research leading to these results has received funding from the European Commission Horizon 2020, the Framework Programme for Research and Innovation (2014-2020), under the grant agreement n° 687500.

VI. REFERENCES

- [1] Rossi A., Alessi E.M., Schettino G., Beck J., Holbrough I., Schleutker T., Letterio F., Vicario de Miguel G., Becedas Rodríguez J., Dalla Vedova F., Stokes H., Colombo C., Gkolias I., Bernelli Zazzera F., Miguel N., Walker S., Romei F., Tsiganis K., Skoulidou D., Stoll E., Schaus V., Popova R., Kim Y., Francesconi A., Olivieri L., Gerardin S., “The H2020 ReDSHIFT project: a successful European effort towards space debris mitigation”, 70th International Astronautical Congress, Washington D.C., USA, 21-25 October 2019, IAC-19.A6.6.4.
- [2] Rossi A. et al., ReDSHIFT: A Global Approach to Space Debris Mitigation, Aerospace , 5, 64, doi:10.3390/aerospace5020064 (2018).
- [3] Letterio F., E.M. Alessi, I. Gkolias, D.K. Skoulidou, V. Schaus, J. Beck, G. Vicario de Miguel, G. Schettino, A. Rossi, C. Colombo, K. Tsiganis, I. Holbrough, N. Miguel, “ReDSHIFT Software Tool for the design and computation of mission end-of-life-disposal”, 7th International Conference on Astrodynamics Tools and Techniques (ICATT), 6-9 Nov. 2018, DLR Oberpfaffenhofen, Germany.
- [4] OPENSF-DMS-SUM-001-36, OpenSF “System User Manual”.
- [5] OPENSF-DMS-OSFI-DM-018, OSFI Developer’s manual.
- [6] Braun V., et al., DRAMA 2.0 – ESA’S SPACE DEBRIS RISK ASSESSMENT AND MITIGATION ANALYSIS TOOL SUITE, 64th International Astronautical Congress 2013, 23-27 September 2013, Beijing, China, paper IAC-13.A6.4.4x18862.
- [7] Klinkrad H., Space Debris. Models and Risk Analysis. Springer, Praxis, 2006. Table 6.1, page 172..
- [8] Urrutxua, H., Sanjurjo-Rivo, M., Paláez, J. “DROMO propagator revisited”. Cel. Mech. Dyn. Astron. 124, p. 1, 2016.
- [9] The Semi-analytic Tool for End of Life Analysis (STELA) has been designed by CNES (The French Space Agency) to support the French Space Operations Act. <https://logiciels.cnes.fr/en/content/stela>.
- [10] Alessi, E. M., Schettino, G., Rossi, A., Valsecchi, G. B. (2018), Natural highways for end-of-life solutions in the LEO region, Cel. Mec. Dyn. Astron. 130, 34.
- [11] Schettino G., Alessi E.M., Rossi A., Valsecchi G.B., Exploiting dynamical perturbations for the end-of-life disposal of spacecraft in LEO, Astronomy and Computing , 27 (2019).
- [12] Rosengren A.J., D.K. Skoulidou, K. Tsiganis and G. Voyatzis, “Dynamical cartography of Earth satellite orbits”, Adv. Sp. Res. 63, p. 443-460, 2019.
- [13] Gkolias I., Colombo C., Towards a sustainable exploitation of the geosynchronous orbital region, Celestial Mechanics and Dynamical Astronomy, 131, 4, 19 (2019).
- [14] Colombo C., de Bras de Fer T., “Assessment of passive and active solar sailing strategies for end-of-life re-entry”, 67th International Astronautical Congress, Guadalajara, Mexico, IAC-16-A6.4.4.
- [15] Alessi, E. M., Schettino, G., Rossi, A., Valsecchi, G. B. (2018), Solar radiation pressure resonances in Low Earth Orbits, Mont. Not. R. Astron. Soc. 473, 2407-2414.
- [16] Skoulidou D.K., A.J. Rosengren, K. Tsiganis and G. Voyatzis, “Medium Earth Orbit dynamical survey and its use in passive debris removal”, Adv. Sp. Res. 63, p. 3646-3674, 2018.
- [17] Gkolias I., Camilla C., (2017) End-of-life disposal of geosynchronous satellites, 68th International Astronautical Congress (IAC) 6, 3613-3619.
- [18] Gkolias I., Camilla C. (2018) Disposal Design for Geosynchronous Satellites Revisited, AAS/AIAA Astrodynamics Specialist Conference, 1-15.
- [19] Colombo C., I. Gkolias I. (2017) Analysis of orbit stability in the geosynchronous region for end-of-life disposal, Proceedings of the 7th European Conference on Space Debris, Darmstadt, Germany.

- [20] Lücking, C., Colombo, C., McInnes, C. R., A passive satellite deorbiting strategy for MEO using solar radiation pressure and the J_2 effect, *Acta Astronautica*, Vol. 77, pp. 197-206, 2012
- [21] Borja, J. A., Tun, D., Deorbit process using solar radiation force, *Journal of Spacecraft and Rockets*, Vol. 43, n°3, pp. 685-687, 2006
- [22] Dalla Vedova, F. et al. Interfacing sail modules for use with space tugs, *Aerospace*, Vol. 5, n° 48, 2018.